Review

Recent Advances in Osmotic Energy Generation via Pressure-Retarded Osmosis (PRO): A Review

Jihye Kim [1], Kwanho Jeong [1], Myoung Jun Park [2], Ho Kyong Shon [2] and Joon Ha Kim [1],*

[1] School of Environmental Science and Engineering, Gwangju Institute of Science and Technology (GIST), 123 Cheomdan-gwagiro, Buk-gu, Gwangju 500-712, Korea;
E-Mails: jihyekim@gist.ac.kr (J.K.); jkh@gist.ac.kr (K.J.)

[2] School of Civil and Environmental Engineering, University of Technology Sydney (UTS), Post Box 129, Broadway, Sydney, NSW 2007, Australia;
E-Mails: Myoung.J.Park@student.uts.edu.au (M.J.P.); Hokyong.Shon-1@uts.edu.au (H.K.S.)

*   Author to whom correspondence should be addressed; E-Mail: joonkim@gist.ac.kr;
Tel.: +82-62-715-3277; Fax: +82-62-715-2434.

Abstract: Global energy consumption has been highly dependent on fossil fuels which cause severe climate change and, therefore, the exploration of new technologies to produce effective renewable energy plays an important role in the world. Pressure-retarded osmosis (PRO) is one of the promising candidates to reduce the reliance on fossil fuels by harnessing energy from the salinity gradient between seawater and fresh water. In PRO, water is transported though a semi-permeable membrane from a low-concentrated feed solution to a high-concentrated draw solution. The increased volumetric water flow then runs a hydro-turbine to generate power. PRO technology has rapidly improved in recent years; however, the commercial-scale PRO plant is yet to be developed. In this context, recent developments on the PRO process are reviewed in terms of mathematical models, membrane modules, process designs, numerical works, and fouling and cleaning. In addition, the research requirements to accelerate PRO commercialization are discussed. It is expected that this article can help comprehensively understand the PRO process and thereby provide essential information to activate further research and development.

1. Introduction

To date, global energy consumption significantly relies on fossil fuels which are closely related to carbon emissions, resulting in an increase of climate change. As such, the exploration of new technologies to obtain energy is increasingly becoming important due to the acceleration of fossil fuel depletion, which has caused apprehension about the available energy supply [1,2]. To meet the ever-increasing energy demands, renewable energy resources such as solar, wind, waves and tidal, biomass, and geothermal sources have been introduced and now share approximately 22% of the total global energy supply [3].

Salinity gradient energy (SGE), which utilizes the chemical potential difference between two solutions having different salinities, has recently gained attention as a promising candidate to reduce the dependence on the fossil fuels. Approximately 0.61 kWh of free energy can be harvested by mixing 1 m^3 of fresh river water and seawater [4]. In addition, the potential of SGE is estimated to be ~2.6 TW, which might make it possible to cover the global energy consumption demands [5]. Other factors that make this technology more favorable include the fact that no emissions of greenhouse gases such as carbon dioxide are produced and there is less dependence on the weather and seasonal conditions compared to renewable energy technologies such as solar and wind energy.

Pressure-retarded osmosis (PRO) is a type of SGE to relieve the energy stress. In PRO, water is transported though a semi-permeable membrane from the feed to the draw side and the pressurized volumetric water flow operates a hydro-turbine to generate power. Although the theoretical concept of harnessing the energy by the mixing of low-saline and high-saline water first was discovered in the early 1950s [6], the specific mechanism was proposed by Loeb in the 1970s [7]. However, PRO has long been considered as economically unfavorable due to its low performance. The use of reverse osmosis (RO) membranes, which were found to be unsuitable for PRO applications, caused severe concentration polarization and finally resulted in a reduction of the overall performances [8]. Based on recent advances in the technological and economic improvement of membrane technologies, PRO has re-emerged as a potentially viable energy option, and lab-scale to pilot-scale demonstrations have actively been conducted. For example, the first PRO pilot plant was constructed by Statkraft in Norway in 2009, and since then several PRO and PRO-hybrid pilot plants have been built or are under construction [9–11]. These facilities include a RO-PRO hybrid pilot plant that was built using a mega-ton water project in Japan, while a RO-MD-PRO hybrid pilot plant was constructed by the global MVP (GMVP) project in Korea. Here, M is for membrane distillation (MD), V is for valuable resource recovery, and P is for PRO. Both projects contribute significantly to advance the PRO process.

In addition, PRO potential and applicability have been intensively investigated in other countries. As an example, the possibility of utilizing PRO in the remote regions of Quebec (Canada) was estimated to have a net energy potential from 0.889 TWh/year to 10.545 TWh/year, according to the site-specific conditions [12]. In Iran, a feasibility study of constructing a 25 MW PRO plant where the Bahmanshir

river meets the Persian Gulf has been investigated [13]. Recently, the feasibility of PRO in Australia was explored based on different combinations of feed and draw solutions by reflecting the source water qualities and the government policies [14]. However, despite this increasing attention and the rapid advancements of the PRO process, several challenges still remain before PRO can reach the commercial stage.

Within this context, the objective of this study is to overview the developments of the PRO process in terms of mathematical models, membrane modules, and process designs. Compared to the recently published review papers [15,16], an emphasis of this study is to provide information on the numerical studies to estimate the feasibility of PRO and PRO-hybrid processes, in conjunction with recent fouling and cleaning studies. Recent advances and progresses of PRO membranes and processes are also extensively updated. Then, the research requirements and directions to further progress PRO commercialization are discussed. Consequently, this review paper can provide comprehensive information to promote the further PRO developments.

2. Theoretical Background

2.1. Characteristics of Osmosis-Driven Processes

Osmosis-driven processes can be divided into three types based on membrane orientation, the existence of hydraulic pressure, and the position of the hydraulic pressure applied. Naturally occurring osmosis has a driving force of forward osmosis (FO) that causes water to be transported through the low-concentrated feed side to the high-concentrated draw side (Figure 1a). Two different operations are possible based on the membrane orientations: an active layer facing the feed solution mode (referred to as the AL-FS mode or FO mode) and an active layer facing the draw solution mode (referred to as the AL-DS mode or PRO mode). The AL-FS mode has more frequently been used in the FO processes since it is less affected by membrane fouling in spite of it having a lower water flux than the AL-DS mode. Research using pressure-assisted osmosis (PAO), which is also referred to as pressurized forward osmosis (PFO) or pressure-assisted FO (PAFO), has recently been proposed that applies the pressure at the feed side in order to further enhance the performance of the FO process (Figure 1b). A pressure ranging from 0 bar to 10 bar has typically been applied in order to increase the water transport while avoiding substantial increases in the energy consumption [17]. In contrast to these two cases, however, a pressure lower than the osmotic pressure difference between the feed and draw solutions is applied at the draw side in the PRO process (Figure 1c).
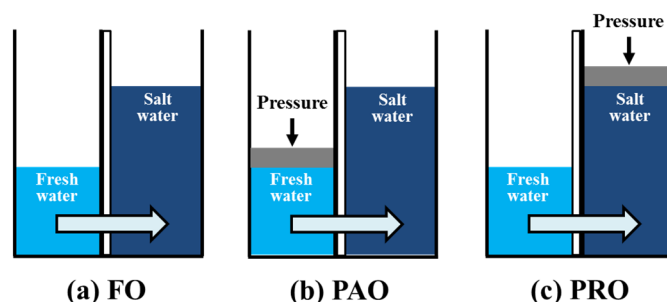

Figure 1. Schematic of osmosis-driven processes: (**a**) forward osmosis (FO); (**b**) pressure-assisted osmosis (PAO); and (**c**) pressure-retarded osmosis (PRO).

2.2. Water Flux and Power Density

Mathematical approaches to describe the water transport in membrane processes, including irreversible thermodynamics models (e.g., Kedem-Katchalsky model and Spiegler-kedem model), pore-based models (e.g., sorption-capillary flow model and pore flow model), and diffusion-based models (e.g., solution-diffusion model and diffusion-adsorption model), were summarized by Soltanieh and Gill in 1981 [18]. Among these models, the solution-diffusion model has been widely used in membrane-based desalination processes, especially in RO, FO, and PRO, which was originally developed by Lonsdale in 1965. Three assumptions are required to employ the solution-diffusion model: (1) the solvent and solute dissolve at the surface of the non-porous membrane; (2) water is solely transported by the diffusion mechanism; and (3) the linear concentration profile should be satisfied [19]. Although the membranes for RO, FO, and PRO are non-porous compared to the porous microfiltration (MF) or ultrafiltration (UF) membranes, they cannot be perfectly pore-free. In this case, not only diffusion but convection may also influence the water transport. Furthermore, if a high-saline solution is used, the linearity of the concentration profile can decrease. Despite the limits, however, the solution-diffusion model is the most common model used to date because of its simplicity.

According to the solution-diffusion model, the water flux is expressed as Equation (1) and becomes Equation (2) based on Henry's law.

$$J_w = -D_w \frac{dc_w}{dx} \tag{1}$$

$$J_w = \frac{D_w c_w}{RT} \frac{d\mu_w}{dx} \approx \frac{D_w c_w}{RT} \frac{\Delta\mu_w}{\Delta x} \tag{2}$$

where J_w is the water flux; D_w is the diffusion coefficient of water in the membrane; c_w is the concentration; x is the axis perpendicular to the membrane surface; R is the gas constant; T is the absolute temperature; and μ_w is the chemical potential as defined in Equation (3). If $\overline{V_w}$ is independent of the pressure, Equation (4) can be derived.

$$\Delta\mu_w = RT \ln \Delta a_w + \overline{V_w} \Delta P \tag{3}$$

$$\Delta\mu_w = -\overline{V_w} \Delta\pi + \overline{V_w} \Delta P = \overline{V_w}(\Delta P - \Delta\pi) \tag{4}$$

where a_w is the chemical activity of water; $\overline{V_w}$ is the partial molar volume of water; P is the hydraulic pressure; and $\Delta\pi$ is the osmotic pressure difference. Then, the water flux can be finally expressed as follows:

$$J_w = \frac{D_w c_w \overline{V_w}}{RT\Delta x}(\Delta P - \Delta\pi) = A(\Delta P - \Delta\pi) \tag{5}$$

where *A* indicates the water permeability described as functions of concentration and temperature.

However, as the osmotic pressure is higher than the hydraulic pressure in PRO, and Equation (6) is typically used to calculate PRO water flux, which makes the value of the positive number.

$$J_w = A(\Delta\pi - \Delta P) \tag{6}$$

As an indicator to evaluate the performance of PRO membranes, the power density is expressed as the product of the water flux and the hydraulic pressure:

$$W = J_w \Delta P = A(\Delta \pi - \Delta P)\Delta P \tag{7}$$

2.3. Concentration Polarizations and Reverse Solute Flux

In the PRO processes, salts are accumulated inside or on the outer surface of the membranes, referred to as the concentration polarization (CP), which consequently plays a negative role on the performance. In general, CP is divided into internal concentration polarization (ICP) and external concentration polarization (ECP) based on the arising position as indicated in Figure 2. The water flux in Equation (6) is further derived as Equation (8) by reflecting the existence of ICP and ECP [20].

$$J_w = A \left[\frac{\pi_{D,b} \exp(-\frac{J_w}{k}) - \pi_{F,b} \exp(J_w K)}{1 + \frac{J_w}{B}\left\{ \exp(J_w K) - \exp(-\frac{J_w}{k}) \right\}} - \Delta P \right] \tag{8}$$

$$K = \frac{S}{D} = \frac{t\tau}{\varepsilon D} \tag{9}$$

where $\pi_{D,b}$ and $\pi_{F,b}$ are the osmotic pressure of draw and feed solutions; k is the mass transfer coefficient; K is the solute resistivity; B is the solute permeability; S is the membrane structure parameter; t is the thickness of the membrane support layer; τ is the tortuosity; ε is the porosity; and D is the diffusion coefficient.

Salts cannot be penetrated through the active layer and eventually are accumulated inside the support layer, causing a concentration increase at the interface of the active layer and the support layer. This phenomenon is referred to as ICP and is described as the term $\exp(J_w K)$ in Equation (8).

The concentration of the draw solution is diluted at the surface of the active layer due to the water transported from the feed side to the draw side, and is referred to as the dilutive ECP. The effect of ECP is presented as $\exp(-\frac{J_w}{k})$ in Equation (8). Although concentrative ECP occurs at the surface of the support layer, it has been ignored because of its relatively low contribution to the membrane performance [21].

In reality, the solute permeates from the high-concentrated draw side to the low-concentrated feed side by diffusion resulting from the rejection rate of the membranes that cannot reach the 100% goal [22]. These reversely transported solutes are accumulated in the support layer and ultimately aggravate the ICP phenomenon. The denominator of Equation (8) denotes the impact of the reverse solute flux and the exacerbated ICP.
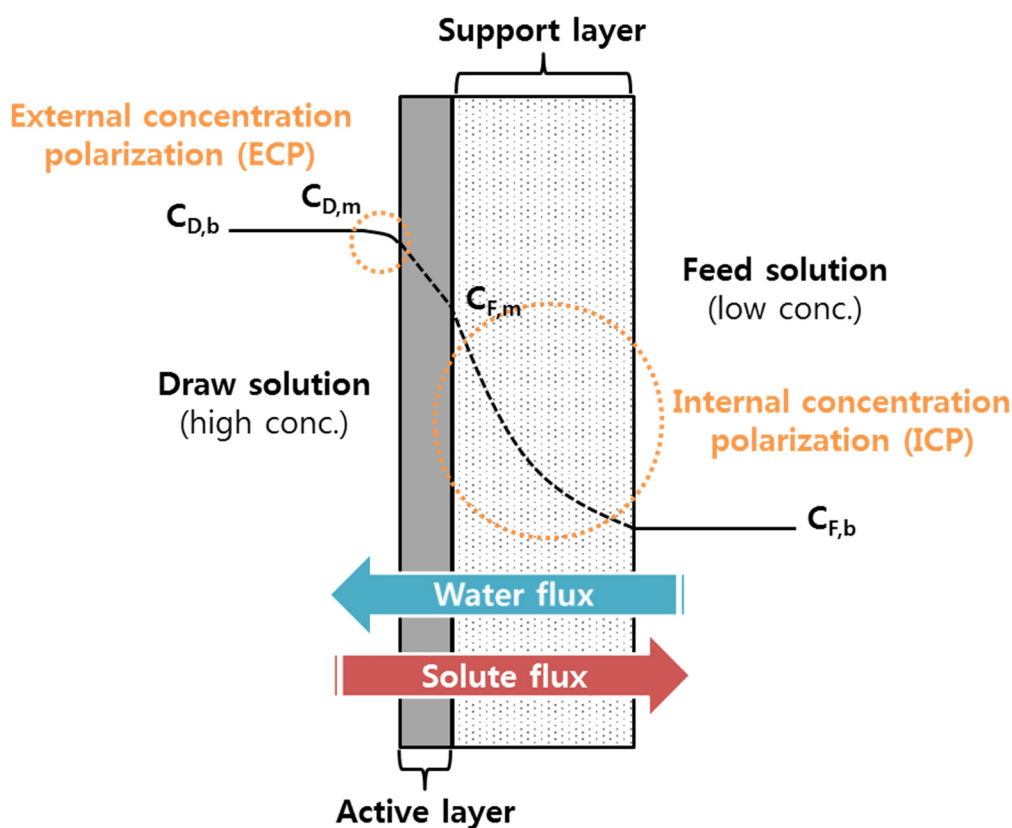
Figure 2. Concentration polarization and reverse solute flux in PRO. $C_{D,b}$ and $C_{F,b}$ are the concentrations of the bulk draw and feed solutions, respectively. $C_{D,m}$ is the concentration at the active layer surface, and $C_{F,m}$ is the concentration at the active layer and support layer interface.

3. Membrane Developments in PRO

RO membranes were used to apply for the PRO evaluations resulting from the non-existence of PRO-specialized membranes at the initial stage of PRO development. Nevertheless, it was found that the RO membranes are not suitable for PRO applications due to the thick support layer which causes severe ICP [8]. Following the rapid improvements on the membrane technology in the 2000s, and the increased focus on SGE, the fabrication of membranes specialized for PRO has actively been conducted worldwide. In this section, the recent developments in the PRO membranes will be discussed by dividing two configurations, e.g., flat-sheet and hollow-fiber membranes.

3.1. Flat-Sheet Membranes

By reflecting the PRO applications, high salt rejection and high water permeability are the key parameters on the membrane developments on PRO. Until the early 2000s, research on the flat-sheet membranes predominantly focused on two materials: cellulose acetate (CA) membranes developed by Loeb in the 1960s, and commercialized cellulose triacetate (CTA) membranes developed and provided by Hydration Technology Innovation (HTI). From the beginning of 2010, thin-film composite (TFC) flat-sheet membranes, mostly composed of two layers (a polyamide (PA) active layer and a highly

porous support layer), are actively being developed due to their advantage on the PRO performance, as compared to a CTA commercial membrane. Compared to the CTA membrane, TFC membranes have a relatively higher salt retention rate due to their thin-film PA selective layer while also having a lower ICP phenomenon, which leads to a higher water flux because of the higher porosity in the support layer. Several research groups in the US and in Singapore have taken leadership positions in developing flat-sheet membranes [23–29]. Table 1 shows the characteristics of notably developed flat-sheet PRO membranes.

The composition of the porous support layer fabricated using non-solvent-induced phase separation to minimize ICP is the basis of technologies developed in 2011 to make PA TFC membranes, with membrane performance being improved with the presence of both finger-like and sponge-like structures in the support layer [23]. In addition, the PRO performances were further enhanced by the modification of the PA active layer in which the power density was improved from 6.09 W/m^2 to 10.0 W/m^2, when the feed and draw solutions were used from river water and seawater, respectively. In 2013, a fully sponge-like structured membrane support consisting of a small structural parameter for the PRO membranes was fabricated and displayed excellent mechanical properties that could withstand a high pressure [24]. To further enhance the PRO performance, the PA layer was modified and the power density increased up to 12 W/m^2 with deionized (DI) water as the feed solution and 1 M NaCl as the draw solution at a hydraulic pressure of 15 bar. A PA-based TFC membrane including a polyacrylonitrile (PAN) support was fabricated, and it was revealed that the increasing PAN concentration and the application of a post-treatment of the support layer by polydopamine coating and ethanol treatment could increase the PRO performance [25]. From the identical group, a power density of 18.09 W/m^2 at 22 bar with the TFC membrane was attained by applying a pre-treatment and post-treatment, adding a surfactant into the interfacial polymerization (IP) solution as a pre-treatment and immersing the membranes in N,N-dimethylformamide (DMF) as a post-treatment [26].

Although the performances of TFC flat-sheet membranes were improved by modifying the support and/or PA selective layer which was fabricated by conventional phase separation technique, their structural parameter (S) values remain high (≥350 μm), which caused severe ICP. Because PRO membranes are required to consist of a high mechanical strength which withstands the hydraulic pressure at the draw side, the sponge-like structure would be a desirable membrane structure. Nonetheless, this morphology normally has a relatively low porosity compared to the finger-like structures. The ideal S value for a PRO membrane is around 150 μm [30]. Thus, in attempts to reduce the S values on PRO membranes, several research groups have developed electrospinning techniques to produce porous membrane support [27–29].

Nanofiber mats as the support layer of TFC PRO membranes produced by electrospinning provide remarkable advantages such as high porosity, low tortuosity, and thin membrane thickness, and these characteristics subsequently decrease the S value. In 2013, an electrospun PAN nanofiber support was first adopted for thin-film nanofiber composite PRO (TNC-PRO) membranes comprising a high mechanical strength and an S value of around 150 μm, which is very close to the ideal value [27]. In 2014, the TFC nanofiber membranes fabricated had a support and two different active layers generated from (1) isophthaloyl chloride and polyethyleneimine and from (2) trimesoylchloride (TMC) and *m*-phenylene diamine (MPD) via IP for NF-like and RO-like TFC PRO membranes, respectively [28]. More recently, a novel TFC membrane composed of a tiered polyetherimide (PEI) nanofiber support

strengthened by functionalized multi-walled carbon nanotubes (f-CNTs) and an ultrathin PA-based active layer was reported [29]. Maintaining a stable power density during 10-hour experiments verified the potential of this membrane for long-term operation. Furthermore, another type of thin-film nanocomposite membrane with f-CNTs in a polyethersulfone (PES) support layer was reported [31]. The increase of the power density up to 110% was exhibited based on the CNT-induced porosity, hydrophilicity of the support layer, and the chemical etching of the PA active layer.

Table 1. Flat-sheet membrane development for PRO.

Name	Material Active/Support	Draw Solution	Feed Solution	Pressure (Bar)	Power Density (W/m^2)	Ref.
PA-PSf TFC	PA/PSf flat-sheet	0.5 M NaCl	40 mM NaCl	12	10.0	[23]
PA-PI TFC	PA/PI flat-sheet	1.0 M NaCl	DI water	15	12	[24]
PAN-TFC	PA/PDA coated PAN flat-sheet	3.5 wt % NaCl	DI water	10	2.6	[25]
TFC-PRO	Modified PA with SDS/PI flat sheet	1.0 M NaCl	DI water	22.0	18.09	[26]
TNC-PRO	PA/modified PAN nanofiber	1.06 M NaCl (Seawater brine)	80 mM NaCl (Synthetic brackish)	15.2	15.2	[27]
TNC-PRO	PA/modified PAN nanofiber	1.06 M NaCl (Seawater brine)	0.9 mM NaCl (Synthetic river)	15.2	21.3	[27]
PAN-mTFC (RO-like)	PA/PAN nanofiber	0.5 M NaCl	DI water	10.3	8	[28]
PAN-pTFC (NF-like)	PA/PAN nanofiber	0.5 M NaCl	DI water	8.6	6.2	[28]
TFC-PRO	PA/CNTs-PEI composite nanofiber	1.0 M NaCl	DI water	16.9	17.3	[29]
TFN-PRO	PA/CNTs-PES	0.5 M NaCl	DI water	6	1.65	[31]

PSf: polysulfone, CNTs: Carbone nanotubes, PI: P84 copolyimide (Matrimid®5218), PDA: Polydopamine, SDS: Sodium dodecyl sulphate.

3.2. Hollow-Fiber Membranes

Hollow-fiber membranes have been developed and are regarded as more attractive than the flat-sheet membranes in terms of real applications due to their high packing density, low footprint, and ease of scale-up [32]. However, unlike flat-sheet membranes, TFC hollow-fiber membranes require a high mechanical strength that could endure a high hydraulic pressure by itself without a backing fabric support. Importantly, these membranes appear to be further developed and optimized for the PRO processes. The fabrication of hollow-fiber membranes specialized for PRO applications started in 2012, led by research teams in Singapore. The representative milestones of PRO hollow-fiber membrane developments are shown in Table 2.

Table 2. Hollow-fiber membrane development for PRO.

Name	Material Active/Support	Selective Layer	Draw Solution	Feed Solution	Pressure (Bar)	Power Density (W/m²)	Ref.
PES-TFC	PA/PES	Lumen side	1.0 M NaCl	10 mM NaCl	8.4	11.0	[32]
PES-TFC	PA/PES	Lumen side	1.0 M NaCl	40 mM NaCl (Waste water brine)	9.0	10.6	[32]
TFC-PEI	PA/PEI	Lumen side	1.0 M NaCl	10 mM NaCl	15.1	20.9	[33]
TFC-PEI	PA/PEI	Lumen side	1.0 M NaCl	10 mM NaCl	15.1	18.7	[33]
PBI-PAN	PBI-POSS/ PAN	Outer layer	1.0 M NaCl	10 mM NaCl	7.0	2.5	[34]
TFC-PI	PA/PI	Outer layer	1.0 M NaCl	DI water	20.0	7.6 (=13.7 [1])	[35]
TFC-PI	PA/PI	Lumen side	1.0 M NaCl	10 mM NaCl	15.0	14.4	[36]
TFC-PI	PA/PI	Lumen side	1.0 M NaCl	40 mM NaCl	15.0	10.6	[36]
TFC-PI	PA/PI	Lumen side	1.0 M Na-Fe-Ca	DI water	12.0	16.2	[37]
TFC-P84	PA/P84	Lumen side	1.0 M NaCl	DI water	21.0	12.0	[38]
PDA-TFC	PA/PDA-PES	Outer layer	0.6 M NaCl	DI water	7.0	3.0	[39]
PDA-TFC	PA-TBP/ PDA-PES	Outer layer	0.6 M NaCl	DI water	8.0	3.9	[40]
PES-TFC	PA/PES	Lumen side	1.0 M NaCl	DI water	20.0	24.3	[41]
PES-TFC	PA/PES	Outer layer	0.6 M NaCl	DI water	6.0	1.6	[42]

PSf: polysulfone, CNTs: Carbone nanotubes, PI: P84 copolyimide (Matrimid®5218); PDA: Polydopamine, SDS: Sodium dodecyl sulphate; [1] The power density is equivalent to its inner-selective (lumen side) hollow-fiber counterpart (*i.e.*, membrane area calculated on the basis of the inner diameter) having the same module size, packing density, and fiber dimensions.

In 2012, a TFC hollow-fiber membrane with a polyethersulfone (PES) support and PA active layer in the lumen side was first introduced [32], and in 2013, the performance was significantly increased by improving the mechanically strengthened support layer fabricated using a PEI polymer to produce TFC PRO membranes [33]. The first hollow-fiber PRO membranes where the active layer was located at the outer layer were fabricated by Chung's research group in Singapore [34,35]. In particular, one was the mixed matrix membrane made from the PBI/polyhedral oligomeric silsesquioxane (POSS) active layer and the PAN/PVP support layer, and another one was a defect-free TFC hollow-fiber membrane produced by the vacuum-assisted interfacial polymerization technique. In 2014, a TFC PRO hollow-fiber membrane having high robustness was designed by controlling the phase separation conditions such as manipulating the composition of the polymer solution and spinning parameters well, and it was tested using different draw solutions such as NaCl and hydro-acid complex draw solutes, denoted as Na-Fe-Ca [36,37]. In addition, the P84 co-polyimide TFC hollow-fiber membrane was developed, and it could withstand a hydraulic pressure up to 23 bar [38]. To increase the power density, modification of the PES-supported membrane using polydopamine (PDA) and then adding tributyl phosphate (TBP) as an additive during the IP was applied [39,40]. PES TFC hollow-fiber membranes consisting of high asymmetry, high porosity, and small pore size distribution were then developed and were found to have

a maximum power density of 24.3 W/m^2 at 20 bar [41]. In order to examine the potential of hollow-fiber membranes for PRO power generation, the influences of operating parameters and the membrane fabrication conditions such as the concentrations of monomers including MPD and TMC and reaction times were subsequently compared [42].

4. Applications in PRO

The concept of harnessing energy from waters with different salinities was first invented by Pattle in 1954 [6]. Then, this technology was intensively studied in the 1970s, led by Loeb, who firstly suggested the terminology of "pressure-retarded osmosis" [7]. In the 2000s, PRO was re-merged due to rapid advances in membrane technology as well as the utilization of a pressure exchanger (PX). In addition, the membrane prices were significantly decreased as a result of advances in membrane development, and the reduction of energy consumption became more likely by applying a PX in PRO, which was originally designed for the RO processes [43]. Based on these break-through events, research on PRO has actively been conducted, from lab-scale to pilot-scale projects. The world's first PRO pilot plant was launched in 2009 in Norway, with several PRO-related pilot plants subsequently being constructed and operated worldwide. Figure 3 summarizes the increased interest in PRO and key developments of the PRO process. In this section, advances in the PRO processes are discussed for two major applications: (1) a stand-alone PRO process and (2) PRO-hybrid processes as the water and energy co-generation process.
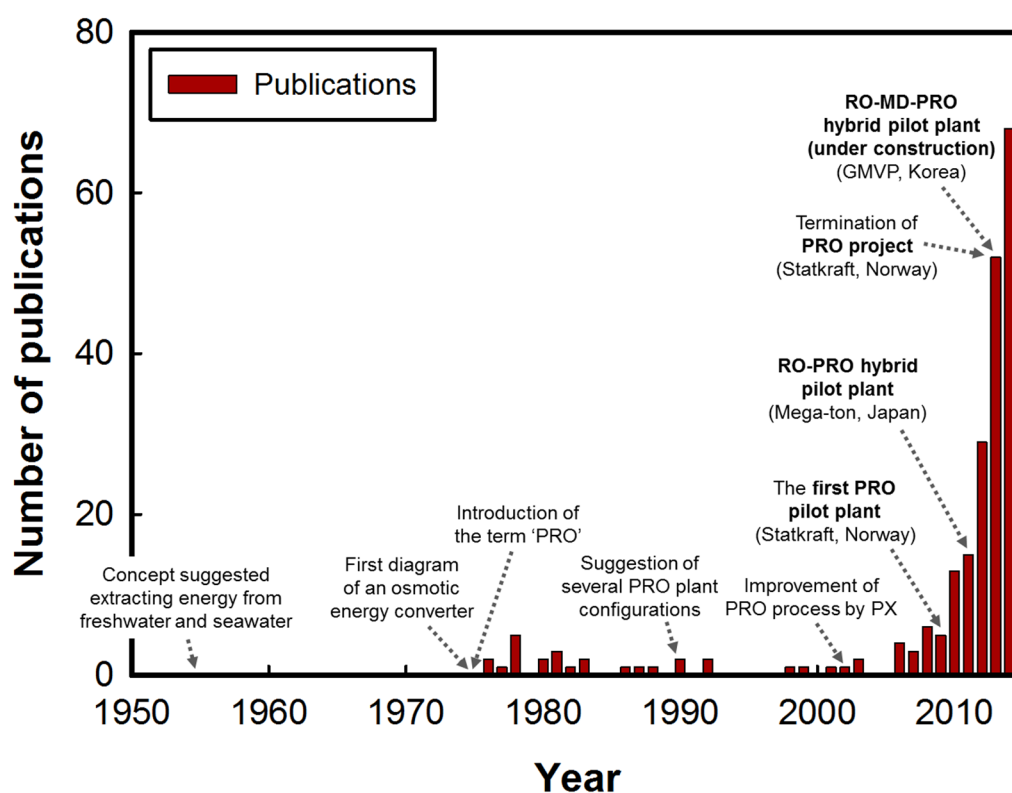

Figure 3. Key developments of the PRO process. Increased attention in PRO is shown by the number of PRO publications collected via Scopus.

4.1. Stand-Alone PRO Processes

A Norwegian power company (Statkraft) that has specialized in hydro power analyzed the economic feasibility of a salinity gradient power in 2008 [9]. Since then, international interests have been drawn to PRO and Statkraft led technological developments in the field. The world's first PRO pilot plant prototype was constructed by Statkraft in Tofte, aiming at producing 10 kW of electricity by pairing river water as a feed solution and seawater as a draw solution (Figure 4). Spiral-wound membrane modules which adopt an effective membrane area of 2000 m^2 and 10–15 bars of the hydraulic pressure were applied, resulting in an average power density of 3 W/m^2. Unfortunately, this value was relatively lower than the power density of 5 W/m^2 required to make PRO economically feasible [9,44]; Statkraft announced the termination of the PRO pilot project at the end of 2012, ahead of the construction of the scaled-up pilot plant (2 MW) [45].
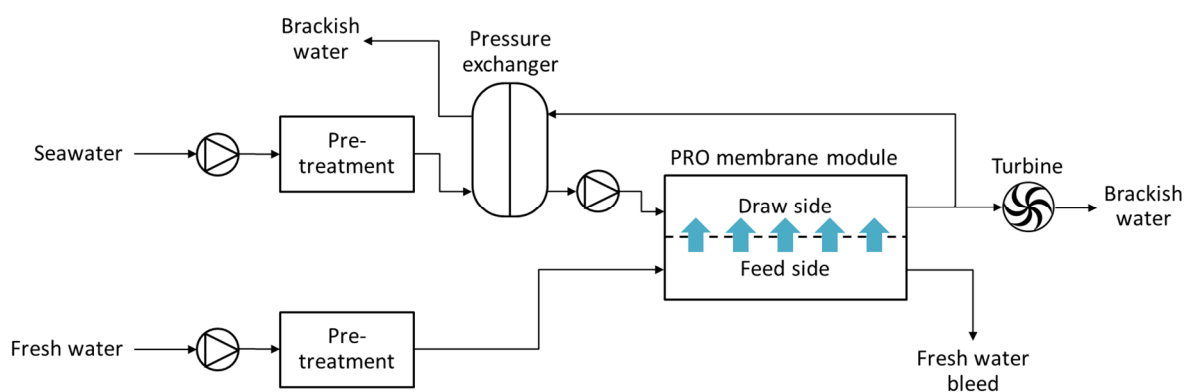

Figure 4. Schematic of Statkraft's PRO pilot plant, adapted from [9].

4.2. PRO-Hybrid Processes

The primary drawback of a stand-alone PRO process is its relatively low power generation, resulting from the low osmotic pressure difference between seawater and river water. If the required energy for pre-treatments is taken into account, the net energy can be further decreased. Based on these considerations, the hybridization of the PRO process with other desalination technologies has actively been investigated. In particular, the RO process is the most preferred option to be coupled with because of advantages such as the alleviation of environmental issues caused by the direct discharge of concentrated brine from RO into the ocean and increasing the PRO power generation by utilizing the high-concentrated brine as a draw solution [46].

A prototype RO-PRO hybrid plant was first constructed in Fukuoka (Japan), as part of the national project named the "Mega-ton Water System". The plant was originally designed by combining RO, PRO, and sewage treatment systems [10] (Figure 5). By utilizing 420 m^3/d of the wastewater effluent as a feed solution and 460 m^3/d of the RO brine as a draw solution, the eight 10-inch hollow-fiber membrane modules from Toyobo were achieved with the maximum power density of 13 W/m^2 at 30 bar of the hydraulic pressure [47]. A scale-up of this RO-PRO hybrid plant is currently being planned in Japan.

Another pilot-scale PRO-hybrid research project has been conducted as the "Global MVP" project in Korea. The objective of this project was to evaluate the feasibility of the RO-MD-PRO hybrid process in terms of reducing the discharged water concentration and the energy consumption. In the hybrid

process, the concentrated RO brine enters the MD feed side, and the further concentrated MD brine is then utilized as a PRO draw solution while the waste water effluent is used as the feed solution (Figure 6). Consequently, improvement of total plant efficiency compared to a stand-alone RO plant is expected due to the additional water production by MD and the reduction of net energy consumption resulting from the PRO energy generation. Specifically, the following pilot plant will be built: a RO system capable of 1000 m^3/d water production, a MD system with a water production capacity of 400 m^3/d, and a PRO system having a 5 W/m^2 power density [11].
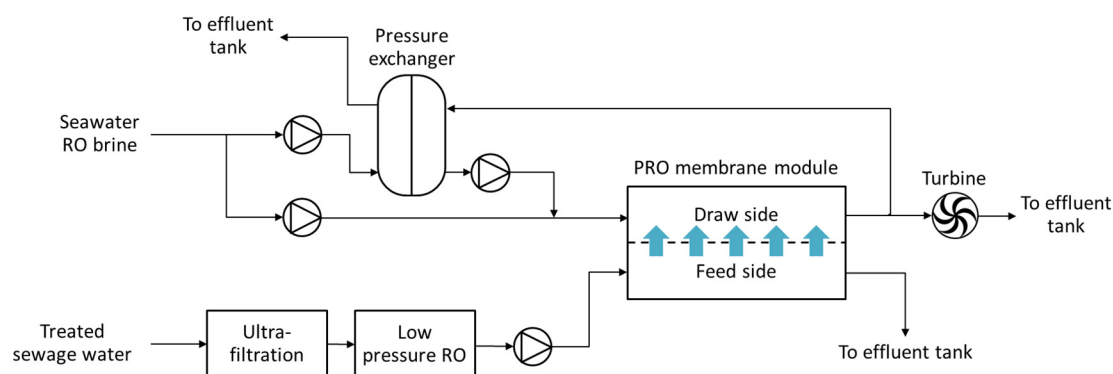

Figure 5. Schematic of the RO-PRO hybrid plant in Japan, adapted from [10].
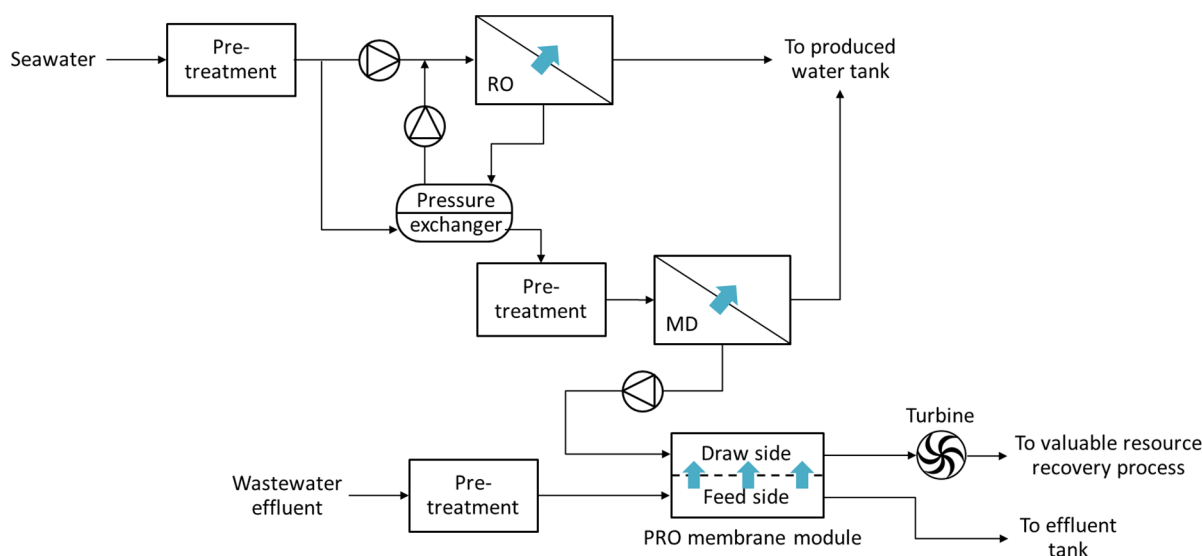

Figure 6. Schematic of the RO-MD-PRO hybrid plant in Korea, adapted from [11].

In the US, Achilli *et al.* [48] reported the experimental results of their RO-PRO small-pilot system, in which they demonstrated the possibility of a PX between the RO and PRO systems (Figure 7). Three 2.8 m^2 spiral-wound RO membrane modules (SW30-2540, Dow Film Tec) and a 4.18 m^2 4040 spiral-wound PRO membrane module developed by Oasys Water were installed. By applying filtered municipal tap water as the PRO feed solution and synthesized seawater as the RO feed water, the average power density of the RO-PRO hybrid system with the PX was reported to be 1.1–2.3 W/m^2. This concept was further developed by Sarp *et al.* [49] and Prante *et al.* [50]. Energy recovery rather than energy production was proposed in their works, obtained by employing the high-pressure diluted PRO draw solution to pressurize the RO feed water via the PX.
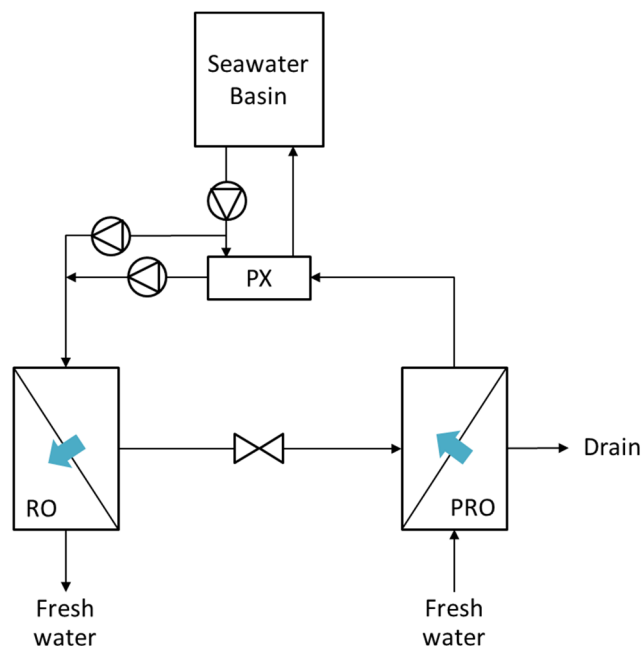
Figure 7. Schematic of the RO-PRO hybrid system in the US, adapted from [48].

Another approach, a closed-loop PRO process referred to as osmotic heat engine (OHE), has been proposed; it is composed of two steps: energy generation and draw solution recovery (Figure 8) [7]. The possibility of utilizing low-grade heat sources such as solar and geothermal energies and biomass heat to re-concentrate the draw solution via the thermal separation stage was regarded as the benefit of the OHE [51]. Further challenges, however, remain before this becomes an economically feasible process. Enhancing the efficiency of the power generation can be achieved by selecting a draw solution that has a high osmotic pressure, high solubility, and high recovery using low-grade heat [52]. Recently, a PRO-MD hybrid OHE system that uses methanol as an organic solvent was suggested in an attempt to improve the thermal separation efficiency of the draw solution [53].
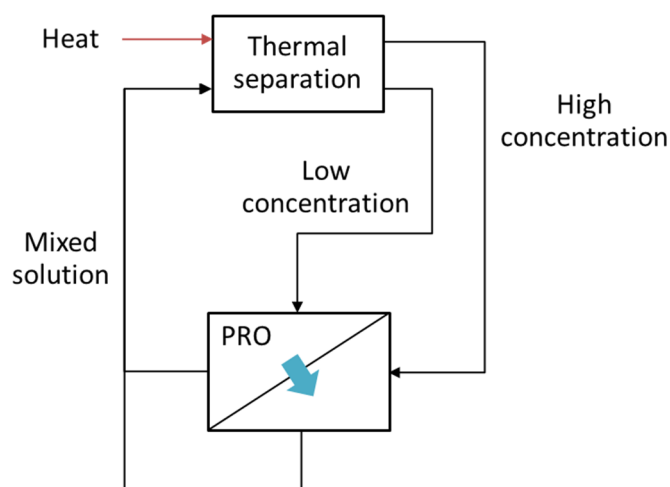

Figure 8. Schematic of osmotic heat engine, adapted from [52].

5. Numerical Studies Regarding PRO

Since Loeb first suggested a mathematical model to simulate the PRO performance in 1976 [54], PRO models have been regarded as a way to additionally consider the effects of ECP, ICP, and reserve solute flux, which were discussed in Section 2 [8,20,21,55]. Recently, these models have been further modified to improve the accuracy of simulating the pilot-scale PRO systems: Kim *et al.* [56] considered the variations of concentration and flow velocities along the membrane channel length, and Naguib *et al.* [57] included the effect of ECP on the feed side, which to date had been ignored in small systems. Table 3 summarizes the noteworthy PRO model developments.

Table 3. PRO model developments.

Author (Year)	Remarks	Ref.
Loeb (1976)	• First PRO model	[54]
Lee *et al.* (1981)	• Consideration of ICP effect	[8]
McCutcheon and Elimelech (2006)	• Consideration of ICP and dilutive ECP (draw side)	[21]
Yip *et al.* (2011)	• Consideration of ICP, dilutive ECP, and reverse solute flux	[20]
Sivertsen *et al.* (2012)	• Modification of the model for hollow-fiber membranes • Consideration of ICP and dilutive ECP	[55]
Kim *et al.* (2013)	• Consideration of ICP, dilutive ECP, and variations of concentrations and velocities along the membrane channel	[56]
Naguib *et al.* (2015)	• Consideration of ICP, dilutive ECP, concentrative ECP (feed side), and variations of the concentrations and velocities along the membrane channel	[57]

As demonstration research on the PRO and PRO-hybrid processes is being actively performed worldwide, interests in numerical studies have been focused on estimating the harnessed energy from PRO by thermodynamic approaches and to simulate the process performances at a large-scale plant to consequently evaluate the economic feasibility of the PRO (Table 4).

The thermodynamic limits of the PRO process under three operation modes (reversible mode, and constant-pressure operation under counter-current flow mode or co-current flow mode) were compared with calculating the extractable specific energy [58]. The maximum specific energy was found to be 0.192 kW/m^3 when pairing seawater (0.6 M NaCl) and river water (0.015 M NaCl), which accounted for 75% of the maximum specific Gibbs free energy. In other studies, the dimensionless approach was newly applied for an ideal counter-flow PRO system to estimate the optimal operating conditions as well as required membrane area [59]. More recently, analysis and optimization of PRO was attempted via a dimensionless parameter referred to as normalized specific energy production, and then the influence of the dilution of draw solution was intensively studied [60]. In the same year, a novel approach to estimate a volumetric energy density of PRO was reported [61]. Based on the method, the maximum achievable specific energy density can be determined by the osmotic pressure and the mass fraction of the feed and draw solutions regardless of the membrane properties.

In addition, an energy and thermodynamic analysis of the single-stage PRO process was conducted by He *et al.* [62], and further, the performance of the dual-stage PRO process under four different configurations was identified [63]. It was found that the configurations of the continuous draw and

continuous feed solution (CDCF) and the continuous draw and divided feed solution (CDDF) were more beneficial than for single-stage PRO processes. The performance of two dual-stage PRO processes was also evaluated by Altaee and Hilal under two different configurations, denoted as an old dual-stage design and a new dual-stage design [64,65]. The difference between the two designs was the partial (old dual stage) or entire (new dual stage) utilization of seawater flow from the first PRO stage, which resulted in a 17.4% increase in the power density achieved with the new design.

In line with trends in process developments, the RO-PRO hybrid configurations have also been favored in numerical research, with four configurations of the RO-PRO hybrid processes being evaluated under various operation pressures of RO and PRO, concentrations of feed and draw solutions, and water and energy prices [56]. The efficiency of the different designs was subsequently compared via a new indicator, the "water and energy return rate (WERR)" (Equation (10)), which can assess the performances of the water and energy co-generation process.

$$WERR = \text{Price}_{Electricity}(\dot{W}_{PRO} - \dot{W}_{Pump}) + \text{Price}_{Water}Q_{P,RO} \tag{10}$$

where $\text{Price}_{Electricity}$ and Price_{Water} are the electricity price and water price, respectively; $\dot{W}_{PRO}$ is the energy generated by PRO; $\dot{W}_{Pump}$ is the rate of work done; and $Q_{P,RO}$ is the volumetric flow rate of the water produced by RO.

The feasibility condition (FC) number (Equation (11)) is another index used to examine the RO-PRO hybrid process, and this number should be >1 in order to operate the hybrid process without utilizing an additional energy source, which can be referred to as a stand-alone RO-PRO hybrid process [66].

$$FC = \frac{\Delta P_{PRO}Y_P}{\Delta P_{RO}Y} \tag{11}$$

where ΔP_{PRO} and ΔP_{RO} are the hydraulic pressures applied to the PRO draw solution and the pressure applied on the RO feed water, respectively; Y_P is the dimensionless water permeation; and Y is the RO water recovery.

Important roles of numerical studies include both the ability to estimate the process performance and to optimize the process. A mixed integer nonlinear programming model-based superstructure optimization was conducted in an attempt to seek an optimal arrangement of the RO-PRO hybrid process by considering the total annual profit of the hybrid system as an objective function [67].

Recently, a new generation of PRO-hybrid processes has been developed. An integrated system of multi-stage vacuum membrane distillation (MVMD) and PRO with a recycling flow scheme (MVMD-R system) was introduced and the performance was evaluated by considering the inlet feed flow rate and the ratio of the recycling flow [68]. In addition, a salinity-solar powered RO (SSRO) system was proposed and its feasibility was compared to that of salinity-powered RO (SRO) processes by using numerical approaches [69].

Table 4. Numerical studies of PRO and PRO-related processes.

Author	Process Type	Remarks	Ref.
Naguib *et al.*	PRO	• Simulate bench-scale and commercial-scale hollow-fiber membranes	[57]
Lin *et al.*	PRO	• Compare thermodynamic limits under different operation modes (reversible, constant-pressure with co-current flow, constant-pressure with counter-current flow)	[58]
Banchik *et al.*	PRO	• Dimensionless analysis for an ideal counter-flow PRO system	[59]
Mingheng Li	PRO	• Model-based analysis and optimization via a dimensionless parameter named as normalized specific energy production	[60]
Reimund *et al.*	PRO	• Pressure-volume analysis to determine the total volumetric energy density regardless of membrane properties	[61]
He *et al.*	PRO (single-stage)	• Energy and thermodynamic analysis of single-stage PRO	[62]
He *et al.*	PRO (dual-stage)	• Performance simulations of dual-stage PRO under four different configurations (CDCF, DDDF, CDDF, DDCF) *	[63]
Altaee and Hilal	PRO (dual-stage)	• Performance simulations of dual-stage PRO under two different configurations (old design and new design) **	[64,65]
Kim *et al.*	RO-PRO hybrid	• Compare performance of RO-PRO hybrid process under four different configurations according to the plant order and feed water concentrations • Develop feasibility indicator for RO-PRO hybrid process: Water and energy return rate (WERR)	[56]
He *et al.*	RO-PRO hybrid	• Diagrammatical analysis of FO-PRO hybrid process • Develop feasibility indicator for RO-PRO hybrid process: Feasible condition (FC) number	[66]
Almansoori *et al.*	RO-PRO hybrid	• Structural optimization of RO-PRO hybrid process via mixed integer nonlinear programming model	[67]
Lee *et al.*	MD-PRO hybrid	• Performance simulation of MVMD-R *** system	[68]
He *et al.*	RO-PRO hybrid, RO-PRO-solar hybrid	• Compare performance between salinity-solar powered RO (SSRO) and salinity powered RO (SRO) processes	[69]

* CDCF: continuous draw and continuous feed solution, DDDF: divided draw and divided feed solution, CDDF: continuous draw and divided feed solution, DDCF: divided draw and continuous feed solution; ** Old design: partial use of seawater from the first PRO stage, New design: entire use of seawater from the first PRO stage; *** MVMD-R: multi-stage vacuum membrane distillation and PRO with recycling flow scheme.

6. Fouling and Cleaning in PRO Processes

6.1. Membrane Fouling in PRO

Fouling occurring in membrane-based water treatment and seawater desalination processes leads to a decrease in the performance of the overall process, such as a reduction in the water flux and an increase of energy consumption. Fouling is classified into organic fouling, inorganic fouling, bio-fouling, and colloidal fouling according to the main foulant. The major mechanisms of fouling include pore narrowing, pore plugging, and cake formation. Pore narrowing occurs when pollutants are absorbed into the internal pore, pore plugging occurs when pollutants plug pores, and cake formation occurs when pollutants pile up onto the membrane surface (Figure 9).
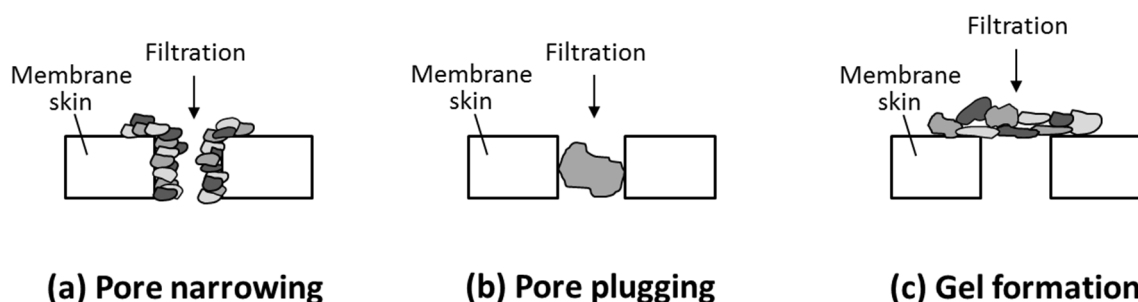

Figure 9. Mechanisms of membrane fouling: (**a**) pore narrowing; (**b**) pore plugging; and (**c**) gel formation.

PRO fouling was initially regarded as less serious since the less-compacted cake layer caused by the lower hydraulic pressure seems to be more easily removed by cleaning processes than for RO [70,71]. PRO fouling, however, should be regarded as an important factor affecting the process performances because AL-DS mode operation (active layer faced draw solution), which is the preferred option for membrane orientation in PRO, may cause severe fouling. Indeed, there is a possibility for foulants to accumulate both outside and inside of the support layer due to the location of the support layer on the feed side. Despite this importance, however, fouling research relating to the PRO processes first appeared in 2013, and requires further rigorous investigation in the future. The PRO fouling research have been conducted to date are summarized in Table 5.

She *et al.* [72] first investigated the impact of the organic fouling in the PRO processes and reported that the fouling could be aggravated by reverse solute diffusion, which was related to the type of draw solution, foulant type, and the intermolecular interaction between the draw solute and foulant. In addition, with regards to natural organic fouling (NOM), Thelin *et al.* [73] investigated the quality of the feed solution and membrane types, while Yip *et al.* [74] examined the influence of the effect of fouling and cleaning by osmotic backwash using their fabricated TFC membranes. In 2014, the scaling caused by calcium sulfate dehydrate (gypsum) was studied by considering the hydraulic pressure, membrane orientation, and types of draw solution and its concentrations [75]. More recently, the influences of the hydraulic pressure and pH on PRO organic fouling were studied by Kim *et al.* [76]. In addition, Kim *et al.* [77] investigated the effect of organic, inorganic, and combined fouling and reported that the support layer was more prone to inorganic fouling, specifically calcium phosphate scaling, due to the reverse solute flux and effects of ICP. In Singapore, real water sources were utilized to identify the extent

of fouling. The power density dropped by approximately 80% when the wastewater effluent from the NEWater plant and seawater RO brine from TuaSpring plant were used [78].

6.2. Membrane Cleaning in PRO

For membrane processes, the methods of physical and chemical cleaning have usually been used to clean fouled membranes. The cleaning efficiency largely depends on the physical (reversible *vs.* irreversible) and chemical (organic *vs.* inorganic) properties of the fouling layer [79]. For instance, in pressure-driven membrane processes, periodic hydrodynamic cleaning can sufficiently mitigate physically reversible membrane fouling without requiring cleaning with strong chemicals, as physical flushing using a high cross-flow velocity easily detaches the deposited foulants from the membrane surface by enhancing the shear rate in a fluid channel [80,81]. Osmotic backwashing (OBW) further enhances the efficiency of physical flushing since the highly compacted fouling layer on the membrane surface becomes loosened by the swelling and lifting effects caused by the naturally driven osmotic backflow, such that the detached foulants are swept out by the physical flushing [82]. These hydrodynamic cleaning methods, however, can be less effective in the PRO processes because organic and inorganic foulants are deposited inside the porous support layer of the membrane. Hence, low shear force is transferred to detach the foulants from the support layer despite the increase of the cross-flow [74,77].

Yip and Elimelech [74] investigated the restoration of permeability from osmotic backwashing for NOM fouling and found that the permeation drag by osmotic backwashing could not completely remove the NOM adsorbed into the active-support layer interface. Recently, the effects of physical flushing, osmotic backwashing, and pressure-assisted osmotic backwashing against inorganic fouling were examined [77]. The beneficial impact of applying a feed solution pre-treatment that has an anti-scalant (e.g., Genesys PHO) was also confirmed, which led to the increase in the solubility of calcium phosphate.

Table 5. Fouling and cleaning studies on PRO processes.

Fouling	Feed solution (Concentration)	Draw Solution (Concentration)	Foulant	Membrane Type	Cleaning Method	Ref.
Organic	10 mM NaCl	$CaCl_2$/NaCl/$MgCl_2$/ Synthetic Seawater (SW)/ Synthetic SW desalination brine (SWBr)	Alginate/ Humic acid	CTA	-	[72]
Organic	Freshwater (Mostadmark water work in Norway)	Synthetic salt water (NaCl + $CaCl_2$ + DI water)	NOM	CTA/TFC	-	[73]
Organic	Synthetic river water (NaCl + $NaHCO_3$ + $CaCl_2$ + DI water)	Synthetic seawater (NaCl solution)	SRNOM	TFC	OBW	[74]
Scaling	Feed solution with bulk gypsum	Synthetic solution ($CaCl_2$/NaCl/Na_2SO_4)	Calcium sulfate dihydrate (gypsum)	CTA	-	[75]
Organic fouling	10 mM NaCl	1.2 M NaCl	Alginate	CTA	-	[76]

Table 5. *Cont.*

Fouling	Feed Solution (Concentration)	Draw Solution (Concentration)	Foulant	Membrane Type	Cleaning Method	Ref.
Organic, inorganic, combined	Synthetic wastewater	Synthetic seawater and its RO brine	Alginate, BSA, SRNOM	CTA	Physical flushing, OBW, Pressure-assisted OBW	[77]
Organic	Wastewater retentate from NEWater plant	SWBr	Effluent organic matter	TFC-PES hollow-fiber membrane	-	[78]

7. Concluding Remarks

The exploration of renewable energy resources is necessary to meet the increasing global energy demands caused by rapid industrialization and population growth. As a promising candidate to relieve the heavy dependence on fossil fuels, PRO has drawn increased attention from academic and industrial communities. Using the salinity gradient between high- and low-saline solutions, PRO can overcome a shortcoming of conventional energy generation technologies and is beneficial to the other renewable energy technologies. For instance, harnessing salinity-gradient energy via PRO ensures no emission of greenhouse gases as well as less periodicity to seasonal and weather variations. In this context, the recent advances of PRO technology are reviewed with regards to theoretical background, membranes, process designs, and numerical studies such as mathematical model development, and simulation and optimization, followed by the recently conducted research specialized in PRO fouling and cleaning.

The current lab-made PRO membranes for both flat-sheet and hollow-fiber types are mostly eligible to meet the economically viable power density of 5 W/m². Demonstration research has been widely conducted in many countries from lab-scale to pilot-scale and is proven to be feasible. Nonetheless, commercial-scale PRO or PRO-hybrid plants have not been operated yet. The following challenges should be addressed in order to further activate the development in PRO technology to reach the commercial stage:

- Development of high-performance PRO membrane module. Outstanding performances in terms of power density have been already achieved by hand-casting membranes. However, to maintain the high performance from small-scale membranes to modules is considered a critical issue. In addition, further enhancement of the PRO membrane and module can be achievable for discovering the new materials or optimizing the membrane parameters [83].
- Selection of adequate pre-treatments with considerations of feed water characteristics. Frequently preferred feed solutions such as wastewater effluent and river water contain various organic and inorganic pollutants, and consequently cause severe membrane fouling. In particular, for the commercial-scale plants, appropriate pretreatments corresponding to water quality characteristics are carefully considered.
- Optimization of the process to enhance the economic feasibility. The efficient configuration of the PRO or PRO-hybrid processes should be suggested site-specific characteristics such as a

plant location, plant capacity, and types of available feed and draw solutions. In addition, optimal operating conditions in terms of the hydraulic pressure, flow rate, temperature, and pH need to be further investigated in order to increase the energy generation of the designed process.

- Improvement of model-based economic analysis. Numerical studies to assess the commercial viability of the PRO process mostly have a critical limitation, *i.e.*, excluding the cost for pre-treatments. To increase the reliability of feasibility studies, the models need to be carefully considered with the effects of all components such as pre-treatments, pumps, membrane modules, PX and hydro-turbine. Furthermore, an indicator that is focused on water and energy co-generation processes is highly required to fairly evaluate the efficiency of the PRO-hybrid processes.

Acknowledgments

Author Contributions

Jihye Kim, Kwanho Jeong, and Myoung Jun Park did the literature review and wrote the paper. Ho Kyong Shon and Joon Ha Kim reviewed and edited the manuscript. All authors read and approved the manuscript.

Conflicts of Interest

The authors declare no conflict of interest.

References

1. Mehio Sibai, A.; Nasreddine, L.; Mokdad, A.H.; Adra, N.; Tabet, M.; Hwalla, N. Nutrition transition and cardiovascular disease risk factors in middle east and north africa countries: Reviewing the evidence. *Ann. Nutr. Metab.* **2010**, *57*, 193–203.
2. Hoffert, M.I.; Caldeira, K.; Benford, G.; Criswell, D.R.; Green, C.; Herzog, H.; Jain, A.K.; Kheshgi, H.S.; Lackner, K.S.; Lewis, J.S.; *et al.* Advanced technology paths to global climate stability: Energy for a greenhouse planet. *Science* **2002**, *298*, 981–987.
3. REN21. Renewables 2014: Global status report. Available online: http://www.ren21.net/ (accessed on 13 July 2015).
4. La Mantia, F.; Pasta, M.; Deshazer, H.D.; Logan, B.E.; Cui, Y. Batteries for efficient energy extraction from a water salinity difference. *Nano Lett.* **2011**, *11*, 1810–1813.
5. Post, J.W.; Hamelers, H.V.; Buisman, C.J. Energy recovery from controlled mixing salt and fresh water with a reverse electrodialysis system. *Environ. Sci. Technol.* **2008**, *42*, 5785–5790.
6. Pattle, R. Production of electric power by mixing fresh and salt water in the hydroelectric pile. *Nature* **1954**, *174*, 660.

7. Loeb, S. Method and Apparatus for Generating Power Utilizing Pressure-Retarded-Osmosis. U.S. Patent 4193267 A, 1975.

8. Lee, K.; Baker, R.; Lonsdale, H. Membranes for power generation by pressure-retarded osmosis. *J. Membr. Sci.* **1981**, *8*, 141–171.

9. Skilhagen, S.E.; Dugstad, J.E.; Aaberg, R.J. Osmotic power—power production based on the osmotic pressure difference between waters with varying salt gradients. *Desalination* **2008**, *220*, 476–482.

10. Saito, K.; Irie, M.; Zaitsu, S.; Sakai, H.; Hayashi, H.; Tanioka, A. Power generation with salinity gradient by pressure retarded osmosis using concentrated brine from swro system and treated sewage as pure water. *Desalin. Water Treat.* **2012**, *41*, 114–121.

11. GMVP. Md/pro Hybrid Desalination Demonstration Plant. Available online: http://www. globalmvp.org (accessed on 10 August 2015).

12. Maisonneuve, J.; Pillay, P.; Laflamme, C.B. Osmotic power potential in remote regions of Quebec. *Renew. Energy* **2015**, *81*, 62–70.

13. Naghiloo, A.; Abbaspour, M.; Mohammadi-Ivatloo, B.; Bakhtari, K. Modeling and design of a 25 MW osmotic power plant (PRO) on bahmanshir river of Iran. *Renew. Energy* **2015**, *78*, 51–59.

14. Helfer, F.; Lemckert, C. The power of salinity gradients: An australian example. *Renew. Sustain. Energy Rev.* **2015**, *50*, 1–16.

15. Helfer, F.; Lemckert, C.; Anissimov, Y.G. Osmotic power with pressure retarded osmosis: Theory, performance and trends—A review. *J. Membr. Sci.* **2014**, *453*, 337–358.

16. Altaee, A.; Sharif, A. Pressure retarded osmosis: Advancement in the process applications for power generation and desalination. *Desalination* **2015**, *356*, 31–46.

17. Sahebi, S.; Phuntsho, S.; Kim, J.E.; Hong, S.; Shon, H.K. Pressure assisted fertiliser drawn osmosis process to enhance final dilution of the fertiliser draw solution beyond osmotic equilibrium. *J. Membr. Sci.* **2015**, *481*, 63–72.

18. Soltanieh, M.; Gill, W.N. Review of reverse osmosis membranes and transport models. *Chem. Eng. Commun.* **1981**, *12*, 279–363.

19. Lonsdale, H.; Merten, U.; Riley, R. Transport properties of cellulose acetate osmotic membranes. *J. Appl. Polym. Sci.* **1965**, *9*, 1341–1362.

20. Yip, N.Y.; Elimelech, M. Performance limiting effects in power generation from salinity gradients by pressure retarded osmosis. *Environ. Sci. Technol.* **2011**, *45*, 10273–10282.

21. McCutcheon, J.R.; Elimelech, M. Influence of concentrative and dilutive internal concentration polarization on flux behavior in forward osmosis. *J. Membr. Sci.* **2006**, *284*, 237–247.

22. Phillip, W.A.; Yong, J.S.; Elimelech, M. Reverse draw solute permeation in forward osmosis: Modeling and experiments. *Environ. Sci. Technol.* **2010**, *44*, 5170–5176.

23. Yip, N.Y.; Tiraferri, A.; Phillip, W.A.; Schiffman, J.D.; Hoover, L.A.; Kim, Y.C.; Elimelech, M. Thin-film composite pressure retarded osmosis membranes for sustainable power generation from salinity gradients. *Environ. Sci. Technol.* **2011**, *45*, 4360–4369.

24. Han, G.; Zhang, S.; Li, X.; Chung, T.-S. High performance thin film composite pressure retarded osmosis (PRO) membranes for renewable salinity-gradient energy generation. *J. Membr. Sci.* **2013**, *440*, 108–121.

25. Zhang, S.; Fu, F.; Chung, T.-S. Substrate modifications and alcohol treatment on thin film composite membranes for osmotic power. *Chem. Eng. Sci.* **2013**, *87*, 40–50.

26. Cui, Y.; Liu, X.-Y.; Chung, T.-S. Enhanced osmotic energy generation from salinity gradients by modifying thin film composite membranes. *Chem. Eng. J.* **2014**, *242*, 195–203.

27. Song, X.; Liu, Z.; Sun, D.D. Energy recovery from concentrated seawater brine by thin-film nanofiber composite pressure retarded osmosis membranes with high power density. *Energy Environ. Sci.* **2013**, *6*, 1199–1210.

28. Bui, N.-N.; McCutcheon, J.R. Nanofiber supported thin-film composite membrane for pressure-retarded osmosis. *Environ. Sci. Technol.* **2014**, *48*, 4129–4136.

29. Tian, M.; Wang, R.; Goh, K.; Liao, Y.; Fane, A.G. Synthesis and characterization of high-performance novel thin film nanocomposite pro membranes with tiered nanofiber support reinforced by functionalized carbon nanotubes. *J. Membr. Sci.* **2015**, *486*, 151–160.

30. Gerstandt, K.; Peinemann, K.-V.; Skilhagen, S.E.; Thorsen, T.; Holt, T. Membrane processes in energy supply for an osmotic power plant. *Desalination* **2008**, *224*, 64–70.

31. Son, M.; Park, H.; Liu, L.; Choi, H.; Kim, J.H.; Choi, H. Thin-film nanocomposite membrane with cnt positioning in support layer for energy harvesting from saline water. *Chem. Eng. J.* **2015**, *284*, 68–77.

32. Chou, S.; Wang, R.; Shi, L.; She, Q.; Tang, C.; Fane, A.G. Thin-film composite hollow fiber membranes for pressure retarded osmosis (PRO) process with high power density. *J. Membr. Sci.* **2012**, *389*, 25–33.

33. Chou, S.; Wang, R.; Fane, A.G. Robust and high performance hollow fiber membranes for energy harvesting from salinity gradients by pressure retarded osmosis. *J. Membr. Sci.* **2013**, *448*, 44–54.

34. Fu, F.-J.; Zhang, S.; Sun, S.-P.; Wang, K.-Y.; Chung, T.-S. Poss-containing delamination-free dual-layer hollow fiber membranes for forward osmosis and osmotic power generation. *J. Membr. Sci.* **2013**, *443*, 144–155.

35. Sun, S.-P.; Chung, T.-S. Outer-selective pressure-retarded osmosis hollow fiber membranes from vacuum-assisted interfacial polymerization for osmotic power generation. *Environ. Sci. Technol.* **2013**, *47*, 13167–13174.

36. Han, G.; Chung, T.S. Robust and high performance pressure retarded osmosis hollow fiber membranes for osmotic power generation. *AIChE J.* **2014**, *60*, 1107–1119.

37. Han, G.; Ge, Q.; Chung, T.-S. Conceptual demonstration of novel closed-loop pressure retarded osmosis process for sustainable osmotic energy generation. *Appl. Energy* **2014**, *132*, 383–393.

38. Li, X.; Chung, T.-S. Thin-film composite P84 co-polyimide hollow fiber membranes for osmotic power generation. *Appl. Energy* **2014**, *114*, 600–610.

39. Ingole, P.G.; Choi, W.; Kim, K.H.; Park, C.H.; Choi, W.K.; Lee, H.K. Synthesis, characterization and surface modification of pes hollow fiber membrane support with polydopamine and thin film composite for energy generation. *Chem. Eng. J.* **2014**, *243*, 137–146.

40. Ingole, P.G.; Kim, K.H.; Park, C.H.; Choi, W.K.; Lee, H.K. Preparation, modification and characterization of polymeric hollow fiber membranes for pressure-retarded osmosis. *RSC Adv.* **2014**, *4*, 51430–51439.

41. Zhang, S.; Sukitpaneenit, P.; Chung, T.-S. Design of robust hollow fiber membranes with high power density for osmotic energy production. *Chem. Eng. J.* **2014**, *241*, 457–465.

42. Ingole, P.G.; Choi, W.; Kim, K.-H.; Jo, H.-D.; Choi, W.-K.; Park, J.-S.; Lee, H.-K. Preparation, characterization and performance evaluations of thin film composite hollow fiber membrane for energy generation. *Desalination* **2014**, *345*, 136–145.

43. Loeb, S. Large-scale power production by pressure-retarded osmosis, using river water and sea water passing through spiral modules. *Desalination* **2002**, *143*, 115–122.

44. Neumann, F. *Report of the Meeting on Salinity Gradient Power Generation*; Institute for Infrastructure, Environment and Innovation (IMI): Brussels, Belgium, 2012; pp. 1–61.

45. Statkraft. Available online: http://www.statkraft.com (accessed on 20 November 2012).

46. Kim, J.; Lee, J.; Kim, J.H. Overview of pressure-retarded osmosis (PRO) process and hybrid application to sea water reverse osmosis process. *Desalin. Water Treat.* **2012**, *43*, 193–200.

47. Kurihara, M.; Hanakawa, M. Mega-ton water system: Japanese national research and development project on seawater desalination and wastewater reclamation. *Desalination* **2013**, *308*, 131–137.

48. Achilli, A.; Prante, J.L.; Hancock, N.T.; Maxwell, E.B.; Childress, A.E. Experimental results from RO-PRO: A next generation system for low-energy desalination. *Environ. Sci. Technol.* **2014**, *48*, 6437–6443.

49. Sarp, S.; In-Ho, Y.; Park, Y.G. Membrane based desalination apparatus with osmotic energy recovery and membrane based desalination method with osmotic energy recovery. Patent WO 2014129724 A1, 2013.

50. Prante, J.L.; Ruskowitz, J.A.; Childress, A.E.; Achilli, A. RO-PRO desalination: An integrated low-energy approach to seawater desalination. *Appl. Energy* **2014**, *120,* 104–114.

51. McCutcheon, J.R.; McGinnis, R.L.; Elimelech, M. A novel ammonia—Carbon dioxide forward (direct) osmosis desalination process. *Desalination* **2005**, *174*, 1–11.

52. Logan, B.E.; Elimelech, M. Membrane-based processes for sustainable power generation using water. *Nature* **2012**, *488*, 313–319.

53. Shaulsky, E.; Boo, C.; Lin, S.; Elimelech, M. Membrane-based osmotic heat engine with organic solvent for enhanced power generation from low-grade heat. *Environ. Sci. Technol.* **2015**, *49*, 5820–5827.

54. Loeb, S. Production of energy from concentrated brines by pressure-retarded osmosis: I. Preliminary technical and economic correlations. *J. Membr. Sci.* **1976**, *1*, 49–63.

55. Sivertsen, E.; Holt, T.; Thelin, W.; Brekke, G. Modelling mass transport in hollow fibre membranes used for pressure retarded osmosis. *J. Membr. Sci.* **2012**, *417*, 69–79.

56. Kim, J.; Park, M.; Snyder, S.A.; Kim, J.H. Reverse osmosis (RO) and pressure retarded osmosis (PRO) hybrid processes: Model-based scenario study. *Desalination* **2013**, *322*, 121–130.

57. Naguib, M.F.; Maisonneuve, J.; Laflamme, C.B.; Pillay, P. Modeling pressure-retarded osmotic power in commercial length membranes. *Renew. Energy* **2015**, *76*, 619–627.

58. Lin, S.; Straub, A.P.; Elimelech, M. Thermodynamic limits of extractable energy by pressure retarded osmosis. *Energy Environ. Sci.* **2014**, *7*, 2706–2714.

59. Banchik, L.D.; Sharqawy, M.H.; Lienhard, J.H. Limits of power production due to finite membrane area in pressure retarded osmosis. *J. Membr. Sci.* **2014**, *468*, 81–89.

60. Li, M. Analysis and optimization of pressure retarded osmosis for power generation. *AIChE J.* **2015**, *61*, 1233–1241.

61. Reimund, K.K.; McCutcheon, J.R.; Wilson, A.D. Thermodynamic analysis of energy density in pressure retarded osmosis: The impact of solution volumes and costs. *J. Membr. Sci.* **2015**, *487*, 240–248.

62. He, W.; Wang, Y.; Shaheed, M.H. Energy and thermodynamic analysis of power generation using a natural salinity gradient based pressure retarded osmosis process. *Desalination* **2014**, *350*, 86–94.

63. He, W.; Wang, Y.; Shaheed, M.H. Enhanced energy generation and membrane performance by two-stage pressure retarded osmosis (PRO). *Desalination* **2015**, *359*, 186–199.

64. Altaee, A.; Sharif, A.; Zaragoza, G.; Hilal, N. Dual stage pro process for power generation from different feed resources. *Desalination* **2014**, *352*, 118–127.

65. Altaee, A.; Hilal, N. Design optimization of high performance dual stage pressure retarded osmosis. *Desalination* **2015**, *355*, 217–224.

66. He, W.; Wang, Y.; Sharif, A.; Shaheed, M.H. Thermodynamic analysis of a stand-alone reverse osmosis desalination system powered by pressure retarded osmosis. *Desalination* **2014**, *352*, 27–37.

67. Almansoori, A.; Saif, Y. Structural optimization of osmosis processes for water and power production in desalination applications. *Desalination* **2014**, *344*, 12–27.

68. Lee, J.-G.; Kim, Y.-D.; Shim, S.-M.; Im, B.-G.; Kim, W.-S. Numerical study of a hybrid multi-stage vacuum membrane distillation and pressure-retarded osmosis system. *Desalination* **2015**, *363*, 82–91.

69. He, W.; Wang, Y.; Shaheed, M.H. Stand-alone seawater RO (reverse osmosis) desalination powered by PV (photovoltaic) and PRO (pressure retarded osmosis). *Energy* **2015**, *86*, 423–435.

70. Thorsen, T.; Holt, T. The potential for power production from salinity gradients by pressure retarded osmosis. *J. Membr. Sci.* **2009**, *335*, 103–110.

71. Chung, T.-S.; Zhang, S.; Wang, K.Y.; Su, J.; Ling, M.M. Forward osmosis processes: Yesterday, today and tomorrow. *Desalination* **2012**, *287*, 78–81.

72. She, Q.; Wong, Y.K.W.; Zhao, S.; Tang, C.Y. Organic fouling in pressure retarded osmosis: Experiments, mechanisms and implications. *J. Membr. Sci.* **2013**, *428*, 181–189.

73. Thelin, W.R.; Sivertsen, E.; Holt, T.; Brekke, G. Natural organic matter fouling in pressure retarded osmosis. *J. Membr. Sci.* **2013**, *438*, 46–56.

74. Yip, N.Y.; Elimelech, M. Influence of natural organic matter fouling and osmotic backwash on pressure retarded osmosis energy production from natural salinity gradients. *Environ. Sci. Technol.* **2013**, *47*, 12607–12616.

75. Zhang, M.; Hou, D.; She, Q.; Tang, C.Y. Gypsum scaling in pressure retarded osmosis: Experiments, mechanisms and implications. *Water Res.* **2014**, *48*, 387–395.

76. Kim, J.; Lee, J.; Kim, S.-H.; Kim, J.H. Impact of hydraulic pressure and pH on organic fouling in pressure retarded osmosis (PRO) process. *Desalin. Water Treat.* **2015**, doi:10.1080/19443994.2015.1043489.

77. Kim, D.I.; Kim, J.; Shon, H.K.; Hong, S. Pressure retarded osmosis (PRO) for integrating seawater desalination and wastewater reclamation: Energy consumption and fouling. *J. Membr. Sci.* **2015**, *483*, 34–41.

78. Wan, C.F.; Chung, T.-S. Osmotic power generation by pressure retarded osmosis using seawater brine as the draw solution and wastewater retentate as the feed. *J. Membr. Sci.* **2015**, *479*, 148–158.

79. Kimura, K.; Hane, Y.; Watanabe, Y.; Amy, G.; Ohkuma, N. Irreversible membrane fouling during ultrafiltration of surface water. *Water Res.* **2004**, *38*, 3431–3441.

80. Yamamura, H.; Kimura, K.; Watanabe, Y. Mechanism involved in the evolution of physically irreversible fouling in microfiltration and ultrafiltration membranes used for drinking water treatment. *Environ. Sci. Technol.* **2007**, *41*, 6789–6794.

81. Boo, C.; Elimelech, M.; Hong, S. Fouling control in a forward osmosis process integrating seawater desalination and wastewater reclamation. *J. Membr. Sci.* **2013**, *444*, 148–156.

82. Qin, J.-J.; Liberman, B.; Kekre, K.A. Direct osmosis for reverse osmosis fouling control: Principles, applications and recent developments. *Open Chem. Eng. J.* **2009**, *3*, 8–16.

83. Sivertsen, E.; Holt, T.; Thelin, W.R.; Brekke, G. Iso-watt diagrams for evaluation of membrane performance in pressure retarded osmosis. *J. Membr. Sci.* **2015**, *489*, 299–307.